Corrosion Science 199 (2022) 110185

Contents lists available at ScienceDirect

Corrosion Science

journal homepage: www.elsevier.com/locate/corsci

Migration of ions on oxygen-deficient chromium oxide electrodeposited from trivalent chromium electrolyte

J. Manoj Prabhakar [a,*], Philipp Kerger [a,b], Arnoud de Vooys [c], Michael Rohwerder [a]

[a] Max-Planck-Institut für Eisenforschung GmbH, Max-Planck-Str. 1, 40237 Düsseldorf, Germany
[b] HYDAC International GmbH, Justus-von-Liebig-Straße 10, 66280 Sulzbach/Saar, Germany
[c] Tata Steel, Research & Development, Ijmuiden Technology Centre, P.O.Box 10.000, 1970CA Ijmuiden, The Netherlands

ARTICLE INFO

Keywords:
Trivalent chromium coating technology (TCCT)
Oxygen adsorption
Scanning Kelvin probe (SKP)
Ambient pressure X-ray photoelectron spectroscopy (APXPS)
Ionic mobility on surfaces and along interfaces
Cathodic delamination

ABSTRACT

The migration of cations on electrodeposited chromium surfaces, with and without a polymer coating, is studied by *in situ* scanning Kelvin probe measurements in an inert atmosphere. The reactivity of the chromium-based coating to the ambient atmosphere is studied using *in operando* ambient pressure X-ray photoelectron spectroscopy in different atmospheres and is shown to have significant impact on cation migration. These findings provide novel and deep insights into ionic mobility at surfaces and along interfaces. Furthermore, an improvement to the conventional cathodic delamination mechanism is proposed based on the outcomes of this study.

1. Introduction

Migration of ions on surfaces and along interfaces plays a crucial role in many electrochemical processes, from sustaining reactions in fuel cells [1,2] and types of atmospheric corrosion such as cathodic delamination [3,4], and they also play an important role in charge dissipation, e.g. during X-ray irradiation studies of insulating samples [5]. Fundamental studies of the underlying processes involved in cation migration on surfaces are rare and focused mainly on the role of fixed charges at the surface or interface [6]. Here, for the case of chromium-based coatings electrodeposited from a trivalent chromium electrolyte, novel insight on the cation migration behaviour on the surface is presented. Electrodeposited chromium-based coatings on steels are widely studied due to their ability to very effectively protect the underlying substrate from wear and corrosion [7]. In the packaging industry, chromium-based coatings were electrodeposited from hexavalent chromium-containing electrolyte until recently. The hexavalent chromium electrolyte is now being eliminated from production processes, for example by the REACH regulations in the EU [8]. A substitute being studied extensively to replace these coatings is a chromium-based coating electrodeposited using trivalent chromium coating technology (TCCT) [9–11]. A recent development in the coatings using TCCT is a coating comprising of two layers, a Cr-O-C layer which is about 10 nm thick and a Cr-O layer (1.5–12 nm thick) on top [9]. These coatings are used in conjunction with a polymer topcoat in the packaging industry, to protect the underlying chromium coated steel from corrosion [11,12]. The adhesion between the polymer topcoat and the substrate will be deteriorated by corrosion processes such as cathodic delamination and filiform corrosion [11,13,14]. Therefore, the resistance of these chromium-based coatings against corrosion driven cathodic delamination of the polymer topcoat [9,10] is of importance, and the two-layered chromium-based coatings were found to provide excellent resistance against cathodic delamination of the polymer coating [9].

Cathodic delamination is widespread, and many concepts are developed to control it, for example, by modifying the surface oxide to retard delamination [15] or using corrosion inhibitors in the polymer layer resulting in self-healing capability [16,17]. The cathodic delamination of organic coatings can be studied by observing the potential changes at the metal/polymer interface using the scanning Kelvin probe (SKP) [3,18–24]. The Kelvin probe is a non-contact technique that measures the corrosion potential on the surface of metal covered with electrolyte or buried under a polymer topcoat [19,25,26]. Cathodic delamination is initiated using an artificial defect and filling it with electrolyte (Fig. 1a). Both anodic and cathodic reactions are fast at the defect, whereas the anodic metal dissolution reaction is extremely slow at the intact metal/polymer interface [27,28]. The defect is characterized by low potentials, indicating active corrosion, and high potentials, characteristic for the passive metal, prevail at the intact metal/polymer

* Corresponding author.
E-mail address: m.prabhakar@mpie.de (J.M. Prabhakar).

https://doi.org/10.1016/j.corsci.2022.110185
Received 30 November 2021; Received in revised form 10 February 2022; Accepted 17 February 2022
Available online 19 February 2022

interface [23]. Oxygen reduction reaction (ORR) can still occur at the intact metal/polymer interface but is inhibited due to the lack of anodic partial reaction in the absence of a bulk electrolyte [23]. When the hydrated ions from the electrolyte reach this interface and establish a galvanic coupling with the defect, oxygen reduction occurs at these locations far from the defect [23,24], sustained by this migration of ions. The accelerated oxygen reduction at the intact interface leads to a cathodic potential shift. The reactive radical intermediates formed during oxygen reduction reaction lead to delamination by destroying the bonding between the surface and polymer [3].

The kinetics of the delamination can be analysed by plotting the position of the delamination front as a function of time and calculating the rate of delamination. A linear dependence of the position of delamination front with time is regarded to result from a charge-transfer controlled process where the oxygen reduction reaction is the rate-limiting step [24,29]. A parabolic dependence where the position of the front follows a square root dependence with time is considered to arise when the delamination process is cation migration rate controlled [18,22]. The migration of ions along the metal/polymer interface is therefore an integral step during the cathodic delamination process.

In oxygen containing atmospheres, the migration of cations on the surface is accompanied by transfer of electrons to support ORR (Fig. 1a). In an inert atmosphere, cathodic delamination is not expected to occur due to the absence of the radicals that result from ORR, that degrades the bonding between the polymer and the surface. The curves of corrosion potential (E) vs the distance to the defect obtained in nitrogen are still similar to that obtained in air, depicting the migration of ions along the surface (as illustrated in Fig. 1b) [3,4]. However, the interface stays intact as no oxygen reduction caused degradation can occur. The sigmoidal curve obtained in nitrogen depicts three distinct regions on the surface: (i) ion-migrated region characterized by cathodic potentials, (ii) non-ion migrated region or intact metal/polymer interface region where anodic potentials are prevalent, and (iii) migration front separating the ion migrated and non-migrated regions where a steep change in corrosion potential is observed. These regions are similar to the (i) delaminated region, (ii) intact region and (iii) delamination front, respectively, expected in the case where oxygen is present in the environment (Fig. 1b).

In situ SKP studies in inert atmosphere provide information about cation migration without any effects from other reactions such as oxygen reduction and degradation of the interface [3,4]. For the chromium coatings studied here this also simulates the low oxygen-containing environment in food packaging where these chromium-based coatings are utilized [11].

The current work aims at understanding the migration of ions on the surface of chromium-based coatings. *In situ* cation migration studies in inert nitrogen atmosphere were carried out on the two-layered chromium-based coatings, with and without polymer topcoat, using the SKP. The cation migration behaviour on the surface of these chromium-based coatings in nitrogen atmosphere is compared with that on a native oxide of chromium. Furthermore, the effect of the cation size on the migration behaviour was studied, too. The role of the atmosphere is twofold. Firstly, in oxygen containing atmosphere, ORR takes place, which might influence the mobility, for instance by the correlated change of pH and for polymer coated samples also by the degradation of the interfacial bonds. Secondly, species such as CO_2 could adsorb on the surface, resulting in the formation of carbonates and/or change of pH and thus have an effect on migration [29–31]. The adsorption of these molecules on the coating surface was hence studied using *in situ* ambient pressure X-ray photoelectron spectroscopy (APXPS) in the presence and absence of oxygen and carbon dioxide. Work function measurements were carried out in vacuum and oxygen environment using APXPS. During APXPS measurements to obtain the work function, an external bias was applied to the sample to obtain the onset of secondary electron emission [32,33]. The results obtained from this study along with the comprehensive characterization of these chromium-based coatings comprising of two layers [9] are used to explain the cation migration on the surface of these chromium-based coatings. Correlating the cation migration behaviour observed in this study to the conventional understanding of the migration kinetics, an improvement to the mechanism of the cathodic delamination process is proposed.

2. Materials and experimental methods

2.1. Chromium coatings electrodeposited from trivalent chromium electrolyte (TCCT)

Samples of the two-layered chromium-based coatings (Cr-O-C layer rich in metallic chromium and an oxygen-rich Cr-O layer) with various Cr-O layer thicknesses were obtained from Tata Steel Packaging Europe. The details regarding the production of these layers and their structural and chemical characterization can be found elsewhere [9]. In brief, the

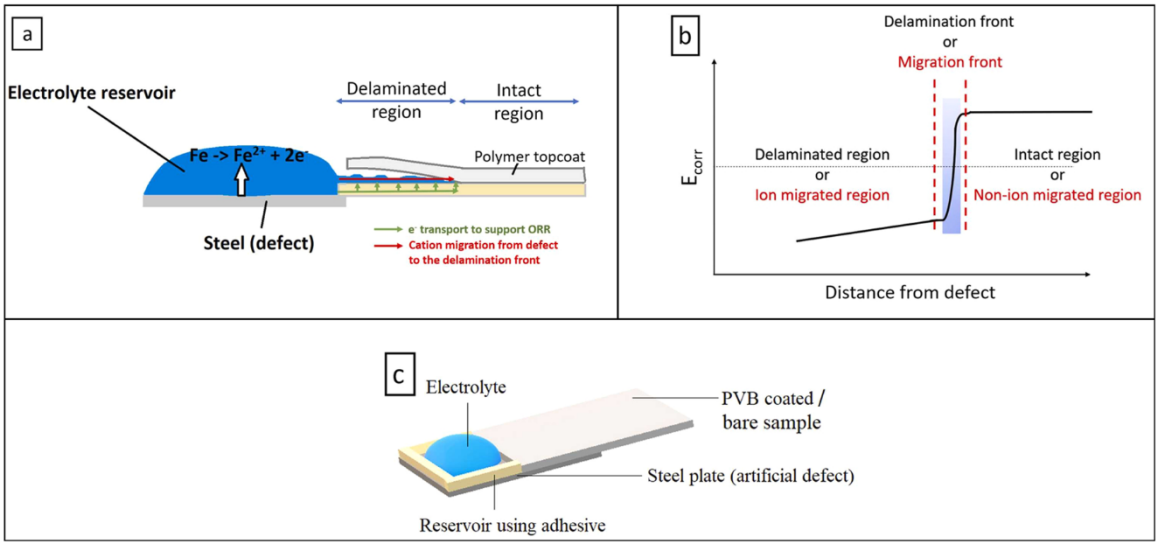

Fig. 1. a) Mechanism of cathodic delamination, b) sigmoidal E vs distance to defect curve obtained during *in situ* cathodic delamination in air (associated regions marked in black) and cation migration studies in nitrogen atmosphere (associated regions marked in red) using a scanning Kelvin probe and c) Schematic drawing of the sample used to study cation migration in nitrogen atmosphere.

Cr-O-C layer (consisting mainly of metallic Cr) is of 10 nm thickness on all the samples. The Cr-O layer thicknesses are 1.5 nm, 6 nm, and 12 nm on the samples 10C-1.5O, 10C-6O, and 10C-12O respectively. The oxygen to chromium ratio in the Cr-O layer was found to be ~1:1, indicating an oxygen-deficient nature [9]. The 10C-1.5O sample with 1.5 nm Cr-O layer was found to consist of native oxide at certain locations on the surface where the thin Cr-O layer was not deposited, due to the oxidation of underlying metallic chromium [9]. Chromium sheets of 99.99% purity and 0.5 mm thickness were purchased from Goodfellow, Germany.

The cation migration measurements using an inert atmosphere in the SKP were carried out on the native oxide on chromium, 10C-1.5O, 10C-6O, and 10C-12O samples. The reactivity of the Cr-O layer to the ambient atmosphere was studied using APXPS on the sample 10C-12O with the thickest Cr-O layer. The influence of different cations on the cathodic delamination rate was compared between the samples with the thinnest and thickest Cr-O layer, 10C-1.5O and 10C-12O respectively.

2.2. Scanning Kelvin probe measurements

The SKP chamber was filled with nitrogen, to perform the cation migration measurements within an inert atmosphere. The samples were cut into 20 mm × 20 mm sheets and coated with 10 wt% polyvinyl butyral (PVB) polymer in ethanol. The polymer coatings were prepared by using a spin coater and cured at 80° C for ten minutes in an induction furnace. 1 M KCl reservoir on steel acted as the artificial defect, which was placed in contact with the polymer-coated sample (as illustrated in Fig. 1c). The electrolyte was contained by forming walls of the reservoir using X60 cold curing adhesive. The setup used for the cation migration measurements comprising of the reservoir and the polymer-coated sample is similar to the one used previously for the cathodic delamination measurements [9]. The setup was placed in the SKP chamber filled with nitrogen to perform the cation migration studies. The measurements were carried out at humid conditions (relative humidity > 90%) to avoid evaporation of the electrolyte, with the help of an external humidification setup. A similar procedure was followed for the bare samples, except the coating of polymer (Fig. 1c). For the studies with a different cation in the electrolyte reservoir, the defect was filled with 1 M LiCl electrolyte.

The Ni-Cr SKP tip (produced in-house [34]) was calibrated before each experiment, against sat. $CuSO_4$ placed in a Cu crucible. On the basis of this calibration, the measured electrode potentials (E) were referred vs the standard hydrogen electrode (SHE). The details regarding the SKP technique used in this work and its fundamental working principle can be found elsewhere [35–37]. Once calibrated, the SKP directly measures the electrode potential of the surface buried under the polymer layer [26,36,37]. The evolution of the electrode potentials with time were recorded across the sample.

2.3. Ambient pressure X-ray photoelectron spectroscopy studies

The reactivity of the Cr-O layer in the 10C-12O sample to the ambient atmosphere was studied using APXPS equipped with a PHOIBOS 150 NAP 2D DLD hemispherical energy analyzer customized equipment from SPECS Surface Nano Analysis GmbH. X-ray photoelectron spectroscopy (XPS) spectra were obtained using an incident photon beam energy of 1486.7 eV corresponding to the Al-Kα emission line. All spectra were obtained using a pass energy of 20 eV and a step size of 0.05 eV. A dwell time of 0.5 s was used throughout all the measurements. For the measurements where the sample was exposed to a controlled gas phase at a certain pressure, the sample was placed in a reaction chamber, where photoelectron spectroscopy was simultaneously performed. The measurements were carried out in a gas phase of 5 mbar under different gas compositions of oxygen and carbon dioxide.

An external bias was applied to the sample using Keithley 617 programmable electrometer, to acquire the onset of secondary electron emission and deduce the work function. The Fermi level and cut-off energy of secondary electrons were measured to obtain the work functions in vacuum and in the presence of 0.5 mbar oxygen, to understand the role of oxygen.

3. Results

3.1. Cation migration studies in nitrogen

Fig. 2a shows the electrode potential (E) as a function of the distance to the defect at various times, for a PVB coated chromium metal surface within a nitrogen atmosphere. Owing to difficulties in obtaining the point of inflection due to the irregular (not sigmoidal) shape of the curves in Fig. 2a, the position of the migration front was assumed as the distance at E = 0.05 V vs SHE. The evolution of the position of the migration front (x_del) with time in nitrogen, is compared with the values of the position of the cathodic delamination front obtained in air [9] in Fig. 2b. The rate of change of this position in air depicts the rate of cathodic delamination and is similar to the rate of cation migration observed in nitrogen (as can be seen in Fig. 2b).

Fig. 3a and b depict a similar analysis of cation migration in nitrogen and cathodic delamination in air for a 10C-1.5O sample. It is evident from Fig. 3b, that the rate of cation migration observed on the 10C-1.5O sample in nitrogen is much lower than the rate of cathodic delamination of PVB on the 10C-1.5O sample in air, unlike in the case of native oxide on chromium where the rates were similar. A similar decrease in the rate of cation migration in nitrogen compared to the rate of cathodic delamination in air is also observed in the samples 10C-6O and 10C-12O (Figs. 4 and 5 respectively). When the atmosphere was switched to nitrogen, the cation migration was virtually stopped in these samples with a thicker Cr-O layer. The cathodic delamination continued at the former rate after the atmosphere was switched back from nitrogen to air (Fig. 5b and c).

It should be noted that the switch to nitrogen is also accompanied by a decrease in the potential values at the regions where the cation migration has not yet taken place. The decrease in potential at these regions is more prominent in the thicker Cr-O samples (Figs. 4a and 5a) than in the 1.5 nm Cr-O samples (Fig. 3a). This decrease in potentials is reversible and returns to original values (Fig. 5b) when the atmosphere is switched back to air.

It should also be emphasized that the kinetics of migration and delamination vary for the different samples. The cation migration and cathodic delamination kinetics for the chromium sample with native oxide follow parabolic kinetics (Fig. 2b). In the case of the thicker Cr-O layered samples, 10C-6O (Fig. 4b) and 10C-12O (Fig. 5c), the cathodic delamination follows linear kinetics and the cation migration is almost completely hindered. For sample 10C-1.5O, the cathodic delamination follows parabolic kinetics, whereas the cation migration in nitrogen follows linear kinetics (Fig. 3b).

To investigate the role of the polymer topcoat on the decrease in migration rate in nitrogen, the measurements in nitrogen were repeated without the polymer topcoat. Such cation migration measurements without the polymer topcoat were carried out previously on iron and zinc, to eliminate the complex surface-polymer interactions [38]. This analysis would reveal if the decrease in the rate of migration emanates from the strong bonding between the polymer and Cr-O surface, which in nitrogen atmosphere is not destroyed by oxygen reduction, albeit this is highly unlikely due to the weak bonding nature of PVB. The results obtained from the measurement of cation migration on bare samples of native chromium oxide, 10C-1.5O and 10C-12O are shown in Fig. 6a–c respectively. In Fig. 6d, the rates of cation migration on these bare samples are compared with the rates of cation migration on the PVB coated samples discussed above. Although the rates of cation migration with and without the PVB layer vary for the sample 10C-1.5O (Fig. 6d), the rates are still much lower than the rate of cathodic delamination of a PVB coating on 10C-1.5O (Fig. 3b). It is evident from the comparison in

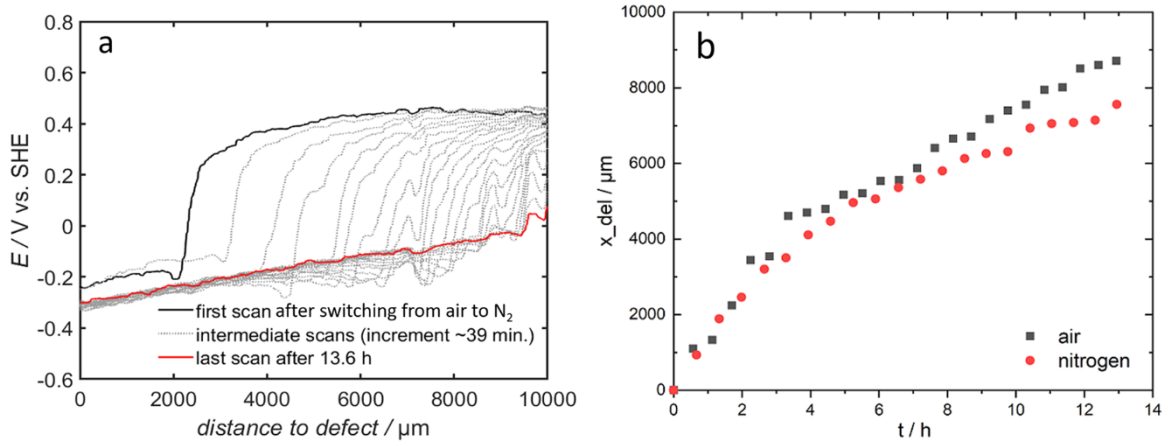

Fig. 2. a) E vs distance to defect curves for cation migration in nitrogen along the interface of native chromium oxide and a PVB coating and b) comparison of the delamination kinetics in air and the migration kinetics in nitrogen for native chromium oxide covered by PVB.

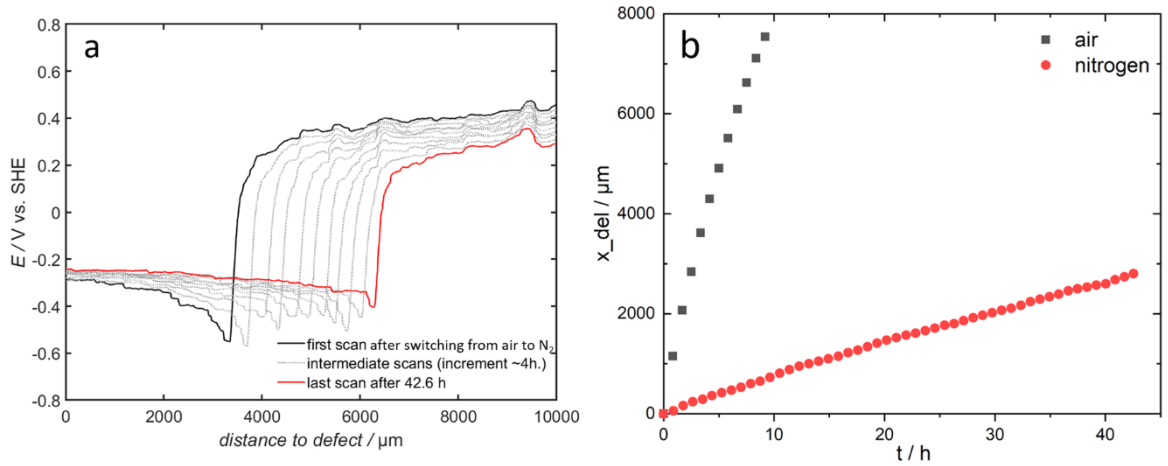

Fig. 3. a) E vs distance to defect curves for cation migration in nitrogen along the interface of 10C-1.5O sample and a PVB coating and b) comparison of the delamination kinetics in air and the migration kinetics in nitrogen for 10C-1.5O covered by PVB. The sharp drop in potential just before the migration front is an artefact of the SKP measurement when the sample is not flat, and has no significant meaning.

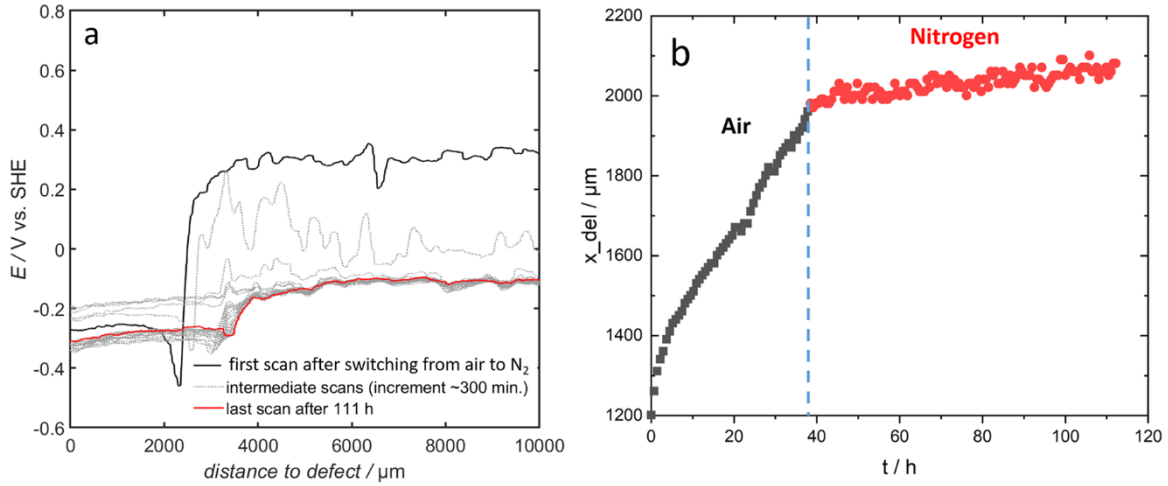

Fig. 4. a) E vs distance to defect curves for cation migration in nitrogen along the interface of 10C-6O sample and a PVB coating and b) comparison of the delamination kinetics in air and the migration kinetics in nitrogen for 10C-6O covered by PVB. The sharp drop in potential just before the migration front is an artefact of the SKP measurement when the sample is not flat, and has no significant meaning.

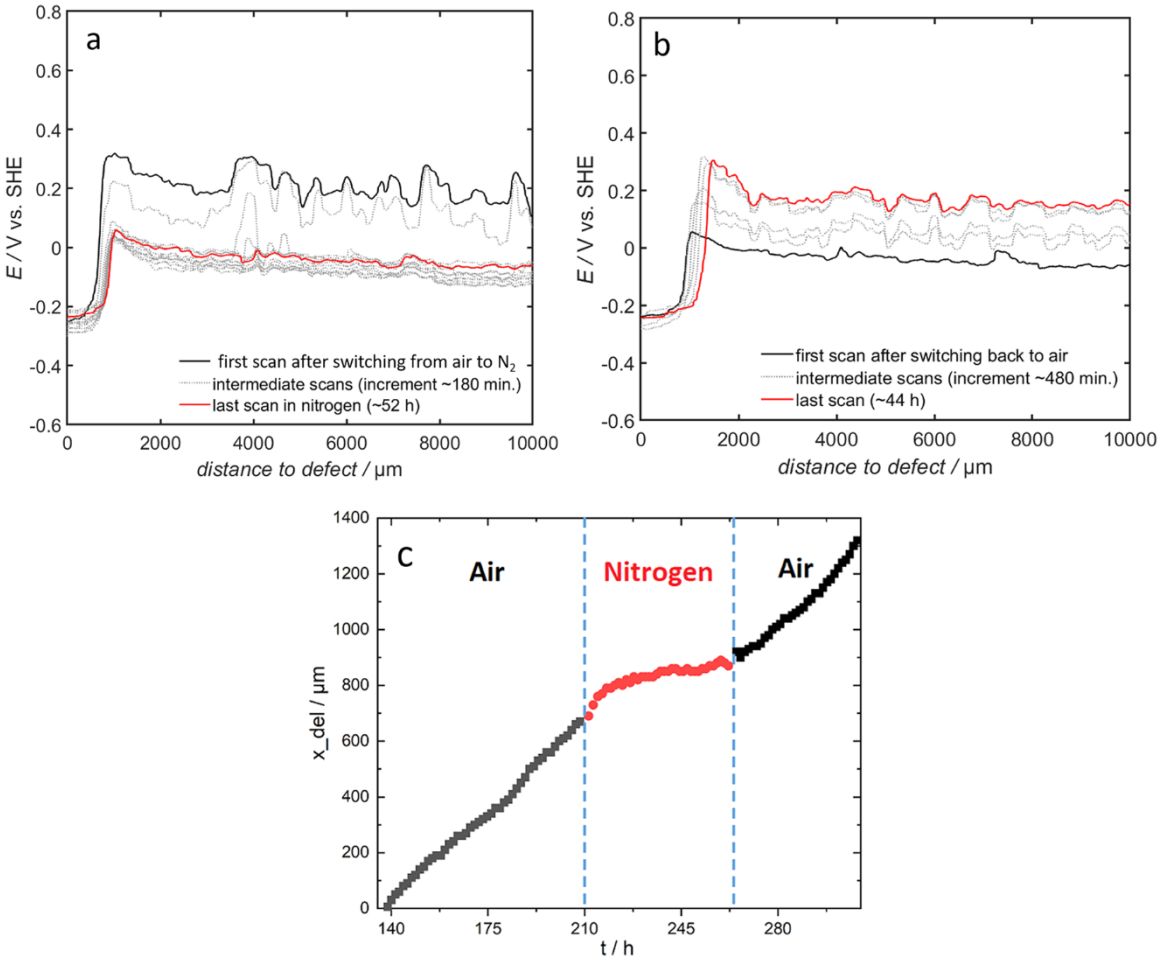

Fig. 5. a) E vs distance to defect curves for cation migration in nitrogen along the interface of 10C-12O sample and a PVB coating, b) E vs distance to defect curves for cathodic delamination along the interface of 10C-12O sample and a PVB coating when switched back to air and c) comparison of the delamination kinetics in air and the migration kinetics in nitrogen for 10C-12O covered by PVB.

Fig. 6d that the PVB layer plays no role in inhibiting the cation migration, and that the rates of cation migration on bare samples are similar to those on PVB coated samples.

3.2. *Ambient pressure X-ray photoelectron spectroscopy measurements*

To determine the role of ambient atmosphere on the Cr-O surface, the sample 10C-12O was analysed using *in situ* APXPS in different atmospheres. CO_2 in the atmosphere has been demonstrated to influence cathodic delamination, ascribed to the formation of carbonates on the surface and affecting the pH and thus the surface charge [29–31], while an effect on the cathodic delamination due to the presence of just adsorbed CO_2 was not discussed. In order to elucidate this in more detail, *in situ* XPS measurements were carried out in the absence and presence of 5 mbar CO_2. Carbon dioxide exhibits an O 1s peak at ~537 eV [39]. The photoelectron spectra from the surface showed no observable change with time, in the presence of CO_2 as revealed by the O 1s spectra obtained on the surface (Fig. 7a). The Cr 2p and C 1s spectra (not shown here) also demonstrated no observable change. The switch from CO_2 to 5 mbar O_2 lead to a clearly visible increase of the Cr-O oxide O 1s peak (Fig. 7b), albeit to no observable changes in the Cr 2p and C 1s spectra. The two peaks at ~539 and 540 eV are attributed to gaseous oxygen, owing to its paramagnetic nature resulting in a core levels split due to the unpaired electrons in the outer orbitals [40,41]. Similar increase of the oxygen peak was also observed when oxygen gas was dosed from ultra-high vacuum to 5 mbar (Fig. 7c). Similar studies on native chromium oxide (not shown here) revealed no pronounced increase as observed in the 10C-12O sample discussed here.

To further investigate the role of oxygen on the Cr-O surface, the work function of the 10C-12O sample was determined in vacuum and the presence of 0.5 mbar oxygen (Fig. 8a and b). Adsorption of oxygen on the surface of the Cr-O and the associated electron transfer from Cr-O to adsorbed oxygen will result in a change in the work function. A change in work function can thus ascertain the adsorption of oxygen on these electrodeposited chromium oxides. From the secondary electron cut-off energy ($E_{cut\text{-}off}$) and the Fermi level (E_F), the work function (φ) can be calculated using the Eq. 1.

$$\varphi = h\upsilon - (E_{cut\text{-}off} - E_F) \quad (1)$$

where $h\upsilon$ is the energy of the incident photon beam (1486.7 eV). The Fermi level does not change when oxygen is introduced in the chamber. However, the binding energy corresponding to the secondary electron cut-off decreases from 1479.57 eV in vacuum to 1478.22 eV in 0.5 mbar oxygen. This corresponds to an increase of 1.35 eV in the work function, in the presence of oxygen.

3.3. *Cathodic delamination studies using different cations*

The results obtained in the cation migration studies carried out in nitrogen atmosphere raise the question in how far the migration observed in nitrogen atmosphere can provide information about the migration rates involved in cathodic delamination occurring in oxygen containing atmosphere. This is because of the significantly reduced

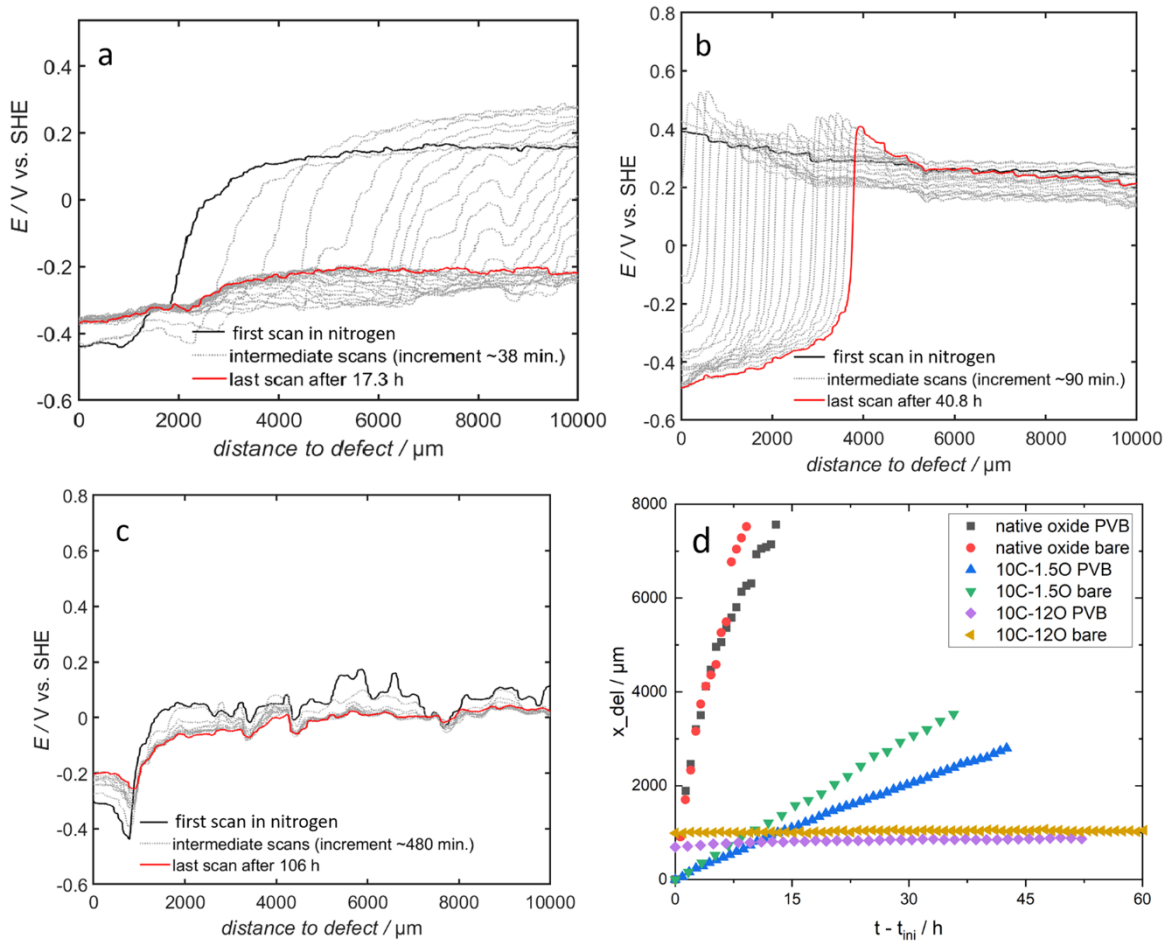

Fig. 6. Cation migration in nitrogen on a bare sample of a) native oxide on chromium, b) 10C-1.5O and c) 10C-12O. The rates observed in PVB coated and uncoated samples are compared in d.

migration rates in nitrogen, as can be especially seen in the significantly hindered cation migration in nitrogen on the thick Cr-O coated samples. In order to further investigate the migration behaviour on the chromium oxide surfaces, measurements were carried out using 1 M LiCl electrolyte in the defect and compared with those using 1 M KCl electrolyte [9]. This served to examine the influence of the size of the cations on the cathodic delamination behaviour. Figs. 9a and 10a depict the evolution of E vs distance to defect curves with time, obtained during cathodic delamination in air, using LiCl electrolyte in the defect, on 10C-1.5O and 10C-12O samples respectively. The plots comparing the delamination kinetics when the defect is filled with LiCl and KCl electrolytes, for the 10C-1.5O and 10C-12O samples are illustrated in Figs. 9b and 10b respectively.

It can be elucidated from Figs. 9b and 10b that the delamination rate on both the samples 10C-1.5O and 10C-12O are influenced by the size of the cation in the electrolyte. In both the samples, the rate of cathodic delamination was lower in the presence of LiCl in the defect, than in the case of KCl in the defect. The delamination of PVB coating on sample 10C-1.5O follows parabolic delamination kinetics both in the presence of KCl and LiCl, whereas the delamination of PVB on sample 10C-12O exhibits linear delamination kinetics in both cases. As mentioned above, linear kinetics are usually associated with oxygen reduction as the rate determining step. However, this should not depend on the size of the cations, while a clear dependence is expected for the case that migration is rate determining. On the other hand, migration as rate determining step is expected to show a sqrt(t) dependence. This will be discussed in the following.

4. Discussions

4.1. Cation migration studies in nitrogen

A comparison of the potential profiles recorded for chromium samples in air and nitrogen (Fig. 2) reveals that the rates of cation migration and cathodic delamination are similar on these samples. This could imply that the migration of the ions is the rate-determining step during the cathodic delamination. It is evident from the cation migration studies in nitrogen that the migration of ions is hindered on the 1.5 nm (Fig. 3), 6 nm (Fig. 4) and 12 nm (Fig. 5) Cr-O coated surfaces. Similar behaviour was observed by Wint et al. on chromium-based coatings consisting only of the Cr-O-C layer, where the migration rate in nitrogen was found to be 0.15 times the cathodic delamination rate in presence of oxygen [11]. It was hypothesized that the observed progress of the potential curves was a continuation of delamination at a decreased rate in nitrogen as consequence of partial reduction of iron, which could be exposed at the surface due to pores in the coating or the iron incorporated in the coating during deposition from trivalent chromium electrolyte [11]. The hypothesis implies that this much less significant iron reduction reaction (of the incorporated iron and that exposed only at the pores) causes a slower progress of cathodic delamination due to a reduced degradation at the interface. However, for the samples used in this study, it has been proved in our previous study that there is no iron incorporation in the Cr-O layer during the electrodeposition process [9]. Hence, the observed progress is that of migration and not delamination.

It was previously reported that the potential difference between the ion migrated and non-ion migrated regions develops in inert atmosphere

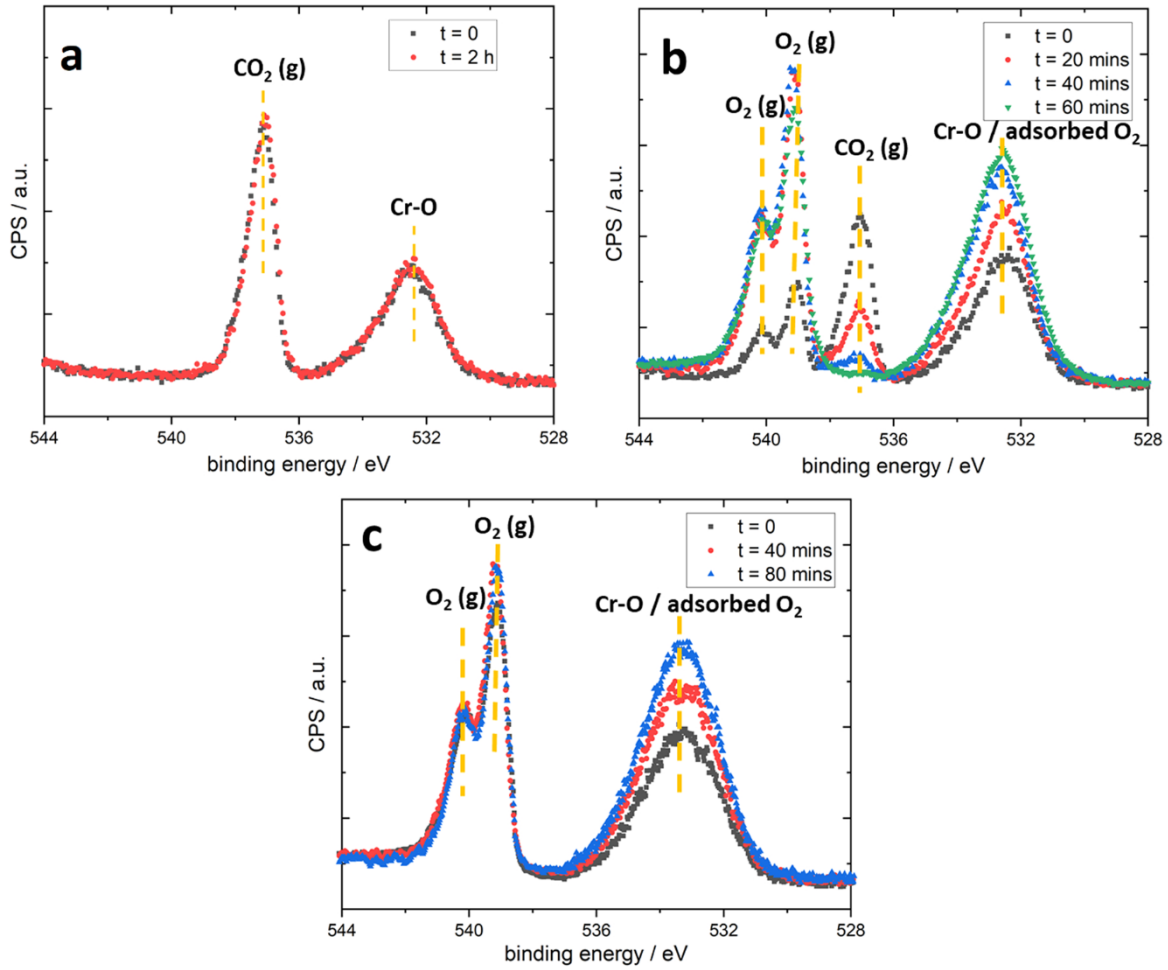

Fig. 7. O 1s spectra on the sample 10C-12O obtained using ambient pressure XPS a) in 5 mbar CO_2, b) after the switch from CO_2 to 5 mbar O_2 and c) after the switch from vacuum to 5 mbar O_2.

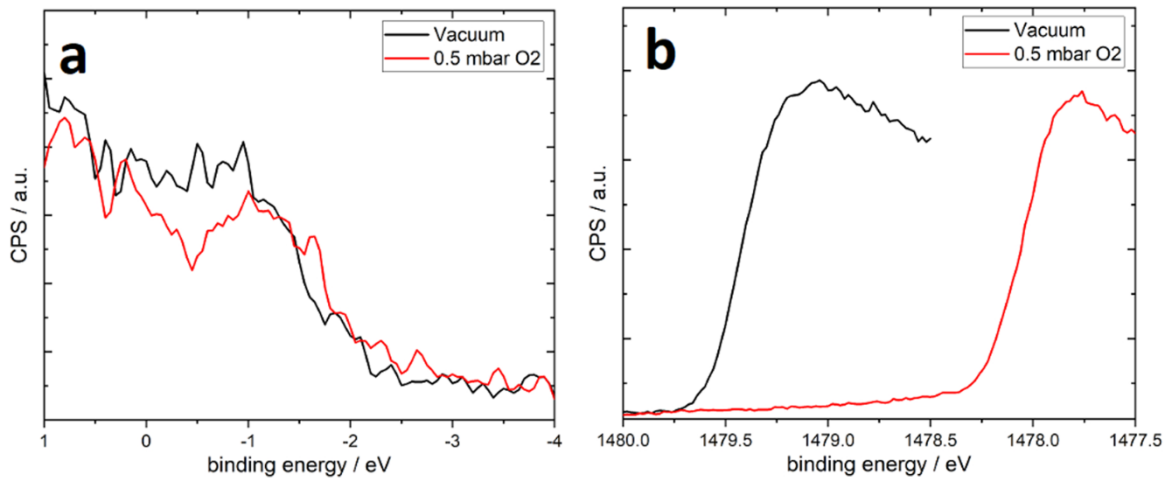

Fig. 8. a) Fermi level region and b) secondary electron emission onset region on the sample 10C-12O in vacuum and the presence of O_2.

even in the absence of a cathodic reaction [3,4,9,18,19]. Driving force is a cathodic polarization at the defect, where the potential is substantially lower than at the interface or on the surface, even in nitrogen. In fact, as long as a potential difference between potential at the defect site and at the intact interface exists, cation migration should occur also in the absence of a cathodic reaction, like in the case of chromium sample with native oxide studied here and in various other substrates [3,4,9,18,19]. Furthermore, as already shown by Leng et al., no meaningful delamination is caused by migration in nitrogen, i.e. no mechanical loss of adhesion is observed in the ion migrated regions where negative potentials prevail [3]. Also, in the current study, the cation migration rate is similar with and without the PVB coating (Fig. 6d). So, it seems

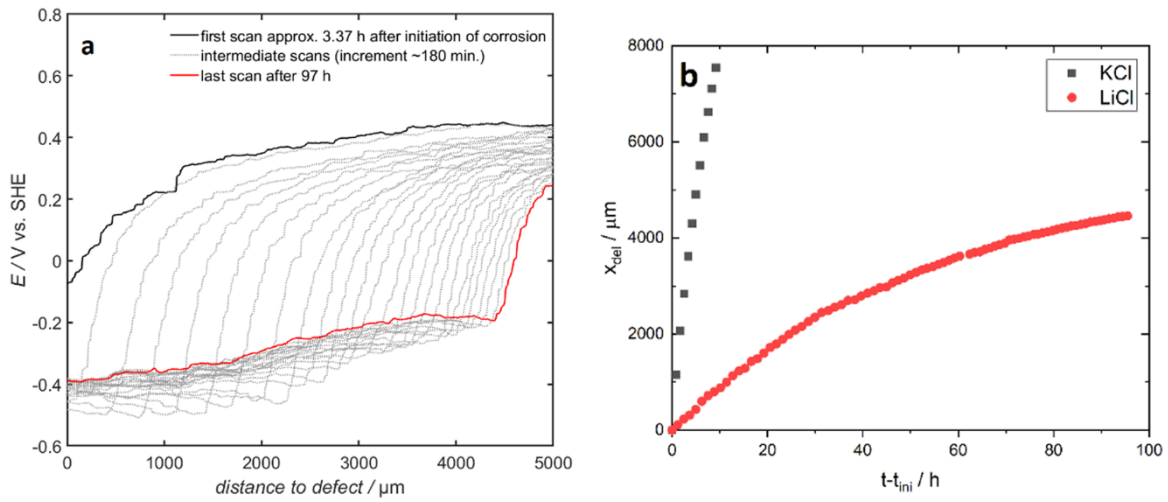

Fig. 9. Cathodic delamination studies using LiCl electrolyte in the defect, on PVB-coated 10C-1.5O sample in humid air a) E vs distance to defect curves and b) comparison of delamination kinetics in the presence of KCl and LiCl electrolytes in the defect.

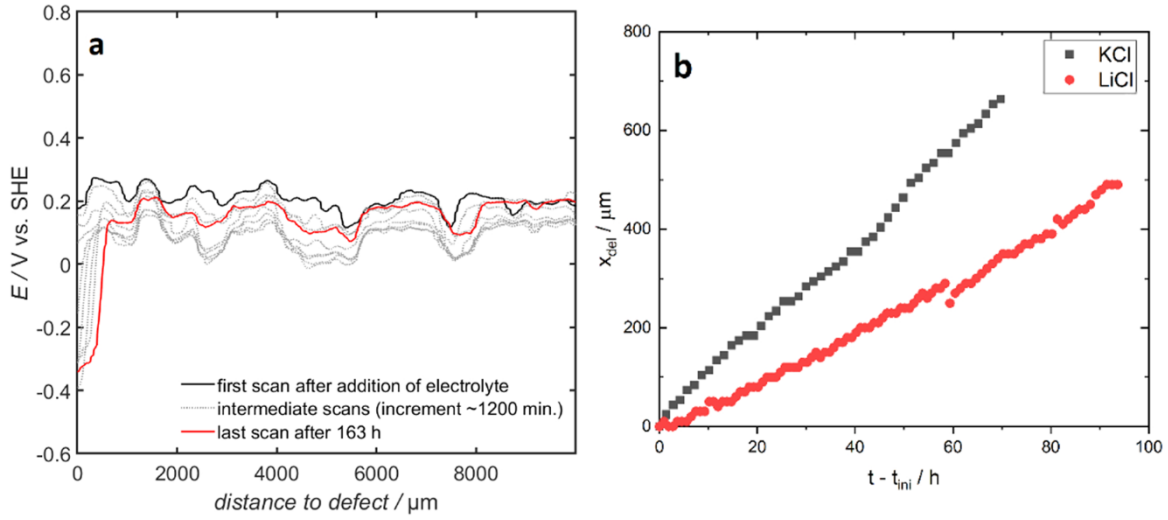

Fig. 10. Cathodic delamination studies using LiCl electrolyte in the defect, on PVB-coated 10C-12O sample a) E vs distance to defect curves and b) comparison of delamination kinetics in the presence of KCl and LiCl electrolytes in the defect.

unlikely that the necessity of ORR and interface degradation by the radicals formed during ORR is the explanation for the higher delamination rate in air compared to the cation migration rate in nitrogen. The difference in the delamination and the cation migration rates seems rather to be correlated to the migration of the cations and it seems that for all samples investigated here the PVB/oxide interfaces do not hinder the cation mobility. Most likely, there is a continuous network of nanopores along the interface where the ions can move on the oxide surface without too much hindrance by the polymer. Hence, it seems that the progress rate of migration/delamination is here determined by the oxide at the surface of the samples and its effect on cation migration. This inhibited cation migration in inert atmosphere appears to be specific to these chromium-based coating surfaces. The property attributed to the inhibition of ions in an inert atmosphere reverts when the atmosphere is switched to air (Fig. 5b).

The switch to nitrogen is also accompanied by a drop in potentials at the non-ion migrated regions. The potential shift could be due to the auto-reduction of the oxide layer [3]. However, such a shift in potential due to the auto-reduction of oxide is mainly specific to metals like iron which can exist in different valence states [3], and not observed in a similar extent if the metal exists in a single valence state. Also, if the drop in potential was observed only due to the auto-reduction of the oxide layer, this would still not explain the diminished cation migration on these surfaces.

The drop in surface potential can also emanate from the desorption of molecules adsorbed from air on the surface of these chromium-based coatings. Adsorption of molecules on the surface results in a change of the work function and thus the electrode potential measured by the Kelvin probe. For instance, adsorption of amino group on metal leads to a negative charge on the surface oxide, reducing the work function for removal of an electron and thus decreases the electrode potential [42]. Similarly, ferrosiloxane bonding leads to a positive charge on the surface of the metal, increasing the electrode potential [42]. The dipole orientation on the surface thus affects the measured electrode potential. The dipole formed due to the adsorption of an electron acceptor molecule results in a positive charge on the surface. This leads to an increase in the work function [43]. This adsorption of molecules in air will be reverted when the atmosphere in the SKP is switched to nitrogen. Therefore, the adsorption of molecules on the surface of these chromium-based coatings was studied using APXPS.

4.2. Adsorption of oxygen on the electrodeposited Cr-O surface

Adsorption of oxygen on the surface of TiO_2 has been studied previously using the shift in binding energies observed in APXPS, emanating from the adsorption and electron transfer process [44]. This gave the idea for a likewise study of the surface of the Cr-O coated steel by using APXPS in the presence of O_2 and CO_2. The XPS O 1s spectra in the presence of CO_2 exhibited no observable change with time (as illustrated in Fig. 7a), eliminating the possibility of adsorption of CO_2 or the formation of carbonates. The O 1s spectra demonstrated strong growth of the oxide peak in the presence of oxygen (as depicted in Fig. 7b and c). A similar investigation in the presence of oxygen was used to elucidate the adsorption of oxygen on the surface of metals [45–48]. Adsorption of oxygen on a clean Fe surface was found to produce a continually growing O 1s peak for increasing oxygen concentrations [45]. Adsorbed $O^{\delta-}$ on the surface was found to produce an O 1s peak in XPS at binding energy similar to the binding energy of hydroxide [46–48]. It was previously shown that the electrodeposited chromium oxides studied here exhibit an O 1s oxide peak at the hydroxide / defective oxide binding energy, owing to their oxygen-deficient nature [9]. It can therefore be elucidated that the growth of the peak here is attributed to the adsorption of oxygen on these chromium-based layers.

Adsorbent molecules can either be classified as electron donors or acceptors based on their electron transfer properties. Oxygen behaves as an electron acceptor [49] and can exist in various ionic and molecular forms when adsorbed on transition metal oxides [50,51]. As discussed earlier, the dipole formed due to the adsorption of oxygen leads to a partially negatively charged species ($O^{\delta-}$) near the surface and a corresponding positive charge on the surface. This leads to increased work function, and Kelvin potentials when measured in air [43]. When the atmosphere is switched to nitrogen, the oxygen molecules desorb, resulting in a decrease in surface potential, explaining the potential changes observed in these chromium-coated samples (Figs. 4a and 5a).

The shift in potentials can also be interpreted in terms of the semiconductive nature of the oxides. These chromium oxides behave like n-type semiconductors since they contain excess metal or are oxygen-deficient [52]. A certain concentration of electrons from the n-type oxide, depending on the defect density, occupy the states that are close to the conduction band minimum (as shown in the flat-band diagram in Fig. 11a). When an acceptor molecule like oxygen adsorbs on the surface of an n-type semiconductor, the electrons are transferred from the semiconductor to the unoccupied molecular orbitals of the acceptor molecule [53,54]. The transfer of electrons leads to upward band bending (as depicted in Fig. 11b) in the space charge region close to the surface of the semiconductor due to the induced electric field [53]. The semiconductor surface is positively charged and the acceptor molecule is negatively charged. The transfer of electrons from the semiconductor to the adsorbed molecule causes an increase in the work function.

The increase in work function associated with the adsorption of oxygen has been ascertained by measuring the Fermi level and secondary electrons cut-off energy level in APXPS. The work function increase is evident as a decrease in the secondary electron cut-off energy. The Fermi level measured in the XPS is not influenced by the adsorption of molecules on the surface and associated changes in the work function [32]. The increase in work function measured in the APXPS (1.35 eV) is higher than the change in Kelvin potentials observed on the 10 C-12 O sample (~0.3–0.4 V). However, it is worth mentioning that the measurements in APXPS are in vacuum and dry O_2, while the measurements in SKP are carried out in very high humidity. The presence of water could explain the difference in the work functions measured using the two different techniques.

The SKP measures the flat band potential of the semiconductor, when there is no change in work function due to adsorbed species changing the surface states. In the case of oxides of iron and zinc, it was found that the increase in electrode potentials measured by the Kelvin probe compared to their flat-band potentials was about 50–100 mV [36]. The higher potential measured by the Kelvin probe compared to reported flat-band potentials is attributed to the adsorption of oxygen on the surface of the n-type oxide, which leads to an upward band bending. In the current work, the adsorption of oxygen results in an electrode potential shift of

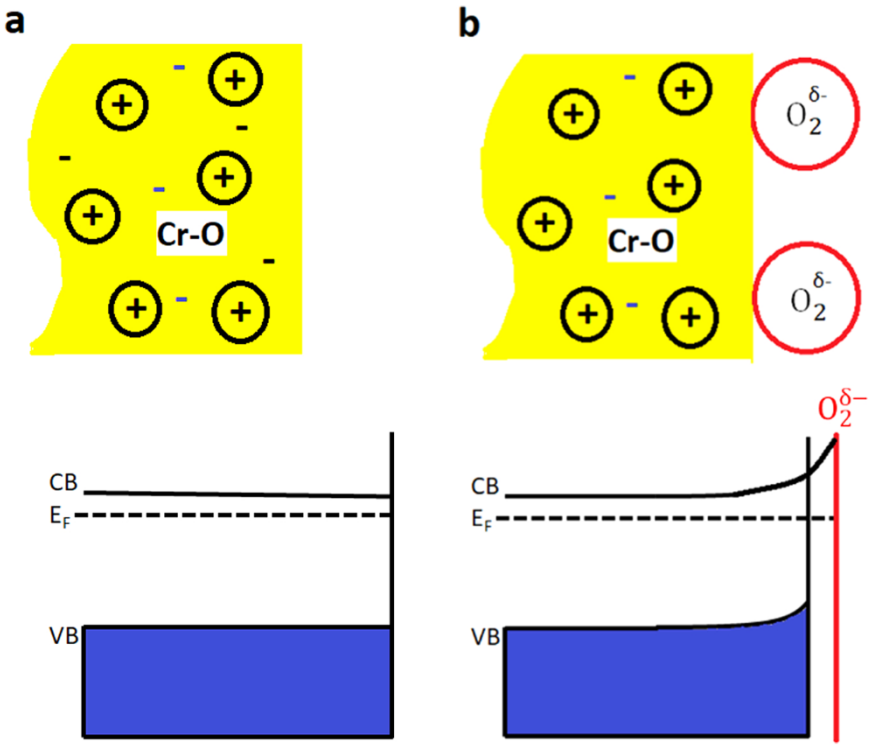

Fig. 11. a) Flat-band diagram and b) band bending observed in the space-charge region of an n-type semiconductor due to transfer of electrons to a donor molecule like oxygen.

~300–400 mV, which could be explained by the highly defective nature of the electrodeposited oxide [9]. This seems to be the reason for an especially high amount of oxygen adsorbing on the surface. It is due to the metastable nature of this oxide that this adsorption does not lead to a healing of the defective structure.

Adsorption of oxygen (acceptor molecule) on TiO_2 has been found to cause a band bending upwards due to the transfer of electrons from TiO_2 to oxygen [44,53–55]. The band bending has been verified to be reversible and diminished on desorption of oxygen using Photoelectron spectroscopy and APXPS [44,53,56]. Similarly, the adsorption on the surface of the chromium-based coatings is reversible as ascertained by the reversal in surface potentials on switching between nitrogen and air (Fig. 5a and b). The upward band bending in the semiconductor separates the electron-hole pairs due to the induced electric field and results in enhanced hole transport or diminished electron transfer to the surface [53,54]. This decrease in electron transport supports the hypothesis of the stifled rate of oxygen reduction which might be one reason for the inhibition of cathodic delamination on the surface of these chromium-based coatings [9]. It is, however, also conceivable that the low cation mobility on this surface is the reason for the slow progress of delamination. However, switching off the effect of ORR to prove this is not possible, since then the surface is changed by the desorption of the adsorbed oxygen, as will be discussed next.

4.3. Cation migration on the electrodeposited Cr-O surface

In situ SKP studies in nitrogen do not only measure the rates of cation migration, but also the associated changes in the properties of the surface in nitrogen. In the chromium-based coatings on steel, the adsorbed oxygen creates a dipole on the surface with a negative charge above the surface and a corresponding positive charge in the Cr-O oxide layer. The oxygen adsorbs preferentially on the electrodeposited Cr-O surface and not that much on the native chromium oxide, due to the oxygen-deficient nature of Cr-O. The Cr-O layer does not entirely cover the underlying metallic chromium in the Cr-O-C layer at low thicknesses, resulting in the formation of native chromium oxide at certain locations on the 10C-1.5O sample [9]. Therefore, the adsorption of oxygen is stronger on the thicker Cr-O layer on the 10C-12O sample, than in the 10C-1.5O sample where oxygen does not adsorb that much on the native oxide (as illustrated in Fig. 12a and b). When switching to nitrogen atmosphere, the oxygen desorbs, which results in a decrease of potential. The decrease in potential is higher for thicker Cr-O layers than for thinner Cr-O layers since the adsorption of oxygen on thinner Cr-O layers is weaker due to native oxide formation at certain locations. The decrease in potentials on switching between oxygen-containing and inert atmospheres were found to indicate the reactivity of a surface towards ORR [57,58]. A higher shift in potential during the gas-switch indicates more changes in the oxide and a higher reactivity of the surface towards ORR. However, in case of the chromium coated steels, the cathodic activity was found to be lower on the thick Cr-O coated surfaces [9] though they portray the largest difference in potentials during the gas-switch. This is because the shift in potentials here is due to the change in work functions subsequent to oxygen adsorption on the surface and do not affect the oxide itself, i.e. no oxidation states or defects are changed.

The adsorption of oxygen on the Cr-O layer also explains the higher mobility of cations in air than in nitrogen. The resultant negative immobile charge on the adsorbed oxygen would lead to anion Donnan expulsion and higher cation mobility on the surface (as depicted in Fig. 12c). On switching the atmosphere to nitrogen, the oxygen on the surface desorbs. Upon switching to nitrogen these fixed negative charges at the surface are lost and thus also the high cation mobility (as depicted in Fig. 12d). In the current study, clear evidence for the adsorption of oxygen has been obtained on the electrodeposited chromium-based coatings. These adsorbed oxygen molecules which are negatively charged, electrostatically attract the cations from the defect. This concept of local electrostatic force stimulated cation migration is of importance not only on these electrodeposited oxygen-deficient Cr-O but most likely on all n-type semiconductor oxides which readily adsorb oxygen or other acceptor molecules.

Cathodic delamination is inhibited at low oxygen partial pressures due to inhibited ORR and thus the absence of radicals to destroy the bonding between the polymer and the surface. From this study, it is evident that the migration of ions on these chromium-based coatings are also inhibited in inert atmospheres or low oxygen partial pressures. These chromium-based coatings are typically utilized in oxygen-depleted environments in the packaging industry [11]. Therefore, the coatings are very suitable for usage in such applications, where the rate of deterioration of the polymer topcoat is highly diminished.

4.4. Cation migration studies using different cations

The influence of the size of the cations on the cathodic delamination behaviour was studied using 1 M KCl and 1 M LiCl in the defect (Figs. 9 and 10). The larger the size of the hydrated cation, the lower its mobility, thus lower the rate of cathodic delamination when delimited by the migration of cations [24,29]. The mobility decreases in the order $Cs^+ > K^+ > Na^+ > Li^+$. A similar trend was also observed during cation migration studies using the SKP in an inert atmosphere [59].

The dependence of the cation size on cathodic delamination is not expected on samples where electron transfer is rate-controlling and linear delamination kinetics is observed [11]. On changing the

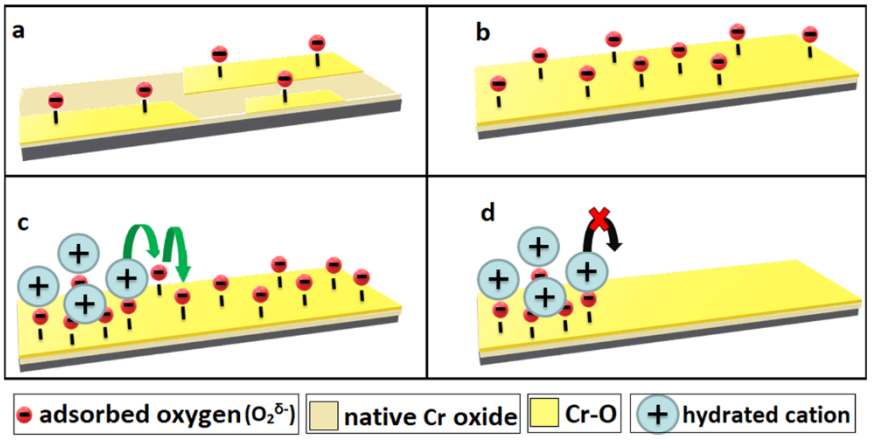

Fig. 12. Adsorption of oxygen illustrated on the surface of the sample a) 10C-1.5O and b) 10C-12O. Migration of ions on the surface of Cr-O coating in c) air and d) N_2.

electrolyte from NaCl to CsCl, no change in delamination rate was observed in a TCCT sample which showed linear delamination kinetics [11]. However, in this study, the sample 10C-12O exhibited different delamination rates in LiCl and KCl, albeit following linear delamination kinetics in both cases. This observation reveals a dependence of the cathodic delamination rate on the size of the cation when cathodic delamination follows linear kinetics. It can thus be elucidated that the process is not necessarily electron-transfer controlled, albeit linear delamination kinetics is observed.

Similarly, it can be elucidated that the parabolic kinetics is not purely due to the process being controlled by cation migration. The 10C-1.5O sample exhibited parabolic dependence with time, both in the presence of LiCl (Fig. 9b) and KCl [9], indicative of a decrease in the delamination rate as the delamination front moves further from the defect. It is noteworthy, that the ohmic (*i*R) drop appears at the delaminated regions in the sample 10C-1.5O with LiCl electrolyte in the defect (Fig. 9a). The ohmic drop is the difference in the electrode potentials of a point just behind the delamination front and a point near the defect. This ohmic drop emanates from the ionic current (*i*) and the resistance to ionic current (R) when the ions migrate from the defect to the delaminated regions and the delamination front. The *i*R drop was previously absent in the cathodic delamination studies with KCl and was hypothesized to be due to lower ionic currents on these chromium-coated steels [9]. However, the potential drop is especially evident in the measurements with LiCl, which can be attributed to the larger size of hydrated cation in Li^+ and thus higher resistance to the ionic transport of Li^+. The difference in potentials between a point just ahead of the delamination front and a point just behind it are usually proposed to be the key driving force for the delamination [4]. The ohmic drop results in a decrease in this driving force as the delamination front moves farther from the defect. This decrease in the driving force with increasing distance from the defect can be the reason for the parabolic kinetics observed and thus, parabolic kinetics need not necessarily imply a cation migration controlled process. Further investigations are needed to emphasize the role of the ohmic drop on the parabolic kinetics observed and is beyond the scope of the current work.

4.5. Cathodic delamination mechanism reconceptualized

In the conventional understanding of the cathodic delamination, the process is considered to be electron-transfer controlled when it follows linear kinetics [24,29] and ion-migration controlled when it follows parabolic kinetics [18,22]. In an ion-migration controlled process, the rate of delamination declines as the delamination front moves further from the defect owing to the larger distance required for cation migration. However, it is more likely that the rate-determining step in the progress of the delamination or migration front is not their migration from the defect to the delamination front, but their progress from a point just behind the front into the intact interface or onto the yet not cation affected surface, as depicted in Fig. 13. This insertion of the cations into a point just ahead of the delamination front from a point just behind it will be influenced by the local electrostatic forces on the cation, the bonding between the substrate and the polymer at the delamination front and the size of the cation, but not on the distance from the defect. This insertion of cations into a point just ahead of the delamination front can be a rate-controlling factor during the cathodic delamination. The proposed mechanism justifies the dependence on the size of cation even when the delamination kinetics follows linear behaviour (Fig. 10) since the insertion will be independent of the distance from the defect. It also explains the linear kinetics in nitrogen observed in the 10C-1.5O sample (Fig. 3b), which indicates no dependence of the migration of ions on the distance from the defect.

5. Conclusions

This study focuses on the migration of ions along the chromium oxide/polymer interface during the cathodic delamination process. The chromium oxides are electrodeposited from trivalent chromium electrolyte and were previously found to be deficient in oxygen compared to the native chromium oxide and to what is thermodynamically expected. The cation migration was studied by switching the atmosphere to an inert gas (nitrogen) and using different cations in the electrolyte during *in situ* scanning Kelvin probe studies. The influence of the ambient atmosphere on the surface of the oxide was studied using APXPS. Based on the results of this study, a modification to the mechanism of cathodic delamination is proposed. The following are the findings of the study:

1. APXPS measurements reveal that the oxygen from the atmosphere adsorbs readily on the surface of these oxygen-deficient chromium oxides. The decrease in surface potential observed in the SKP due to the decrease in the work function of these oxides upon switching to nitrogen also confirms the adsorption of oxygen in air and its desorption in nitrogen atmosphere. The gas switch experiments in SKP, from air to nitrogen and vice-versa reveal that the adsorption of oxygen on the surface of these oxides is reversible. Contrary to what is usually found, the large change of the potential upon switching between air and nitrogen is not related to a high reactivity towards ORR. Such gas switch measurements in SKP do not only measure the cation migration kinetics but also the associated changes in the properties of the surface due to the gas switch.
2. The negative charges on the surface accompanying the oxygen adsorption were found to enhance cation transport on the surface in air. On the contrary, the migration of cations was hindered drastically in an inert atmosphere. These chromium-based coatings on steels are applied in the packaging industry in oxygen-deficient environments. Therefore, these coated steels are suitable for such applications, due to cation transport and thus the cathodic delamination being highly inhibited at these application conditions.
3. For the samples investigated here, the migration of ions on the surface of the bare and the PVB-coated surfaces were found to demonstrate similar kinetics. Thus, the polymer coating played no role in the inhibition of cation migration on these oxide surfaces, most likely because of the presence of a network of nanopores along the interface wherein cations could move on the surface unhindered by the polymer.

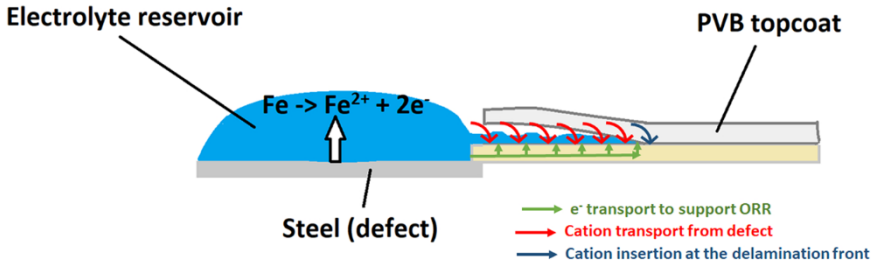

Fig. 13. Improved mechanism of cathodic delamination proposed from the results obtained in this study.

4. The size of cations in the electrolyte was observed to influence the rate of cathodic delamination in both 1.5 nm Cr-O coated and 12 nm Cr-O coated samples. Therefore, neither of the samples portray a purely electron-transfer controlled cathodic delamination process. According to the widely accepted understanding of the cathodic delamination process, which states that linear kinetics should be determined by ORR, the cathodic delamination in the sample 10C-12O which exhibits linear delamination kinetics should not be influenced by the size of the cation, but the results presented here show that it is.
5. The results reveal that the ion transport on the surface does not always follow a parabolic dependence with time and that a linear dependence on time does not mean a purely electron-transfer controlled process. Based on the observations, it is proposed that the insertion of the cations from the delamination front to a point just ahead of the delamination (or migration) front is possibly a rate-determining step. This insertion of cations ahead of the front depends on the size of the cation and is independent of the distance from the delamination front, and thus renders linear delamination kinetics. This step is in fact the first step in the migration or delamination process, as it is the pre-requisite for lowering the potential. Obviously, there is a difference between moving along a delaminated interface or an interface where already cations have migrated into and the intact interface or surface without migrated cations yet. It is proposed that the insertion of the first cations into the intact interface/original surface is kinetically hindered. The insertion of the cations incorporates the influence of local electrostatic forces acting on the cation.

CRediT authorship contribution statement

Manoj Prabhakar: Conceptualization, Methodology, Formal analysis, Investigation, Writing – original draft, Writing – review & editing, Visualization. **Philipp Kerger:** Investigation, Writing – review & editing. **Arnoud de Vooys:** Resources, Supervision. **Michael Rohwerder:** Conceptualization, Funding acquisition, Supervision, Writing – review & editing.

Declaration of Competing Interest

The authors declare that they have no known competing financial interests or personal relationships that could have appeared to influence the work reported in this paper.

Data Availability

The raw/processed data required to reproduce these findings cannot be shared at this time due to legal or ethical reasons.

Acknowledgements

This work is funded by Tata Steel, Netherlands Ijmuiden through IMPRS-SurMat program.

References

[1] X. Zhong, M. Schulz, C.H. Wu, M. Rabe, A. Erbe, M. Rohwerder, Limiting current density of oxygen reduction under ultrathin electrolyte layers: from the micrometer range to monolayers, ChemElectroChem 8 (2021) 712–718, https://doi.org/10.1002/celc.202100083.
[2] H.A. Gasteiger, S.S. Kocha, B. Sompalli, F.T. Wagner, Activity benchmarks and requirements for Pt, Pt-alloy, and non-Pt oxygen reduction catalysts for PEMFCs, Appl. Catal. B Environ. 56 (2005) 9–35, https://doi.org/10.1016/j.apcatb.2004.06.021.
[3] A. Leng, H. Streckel, K. Hofmann, M. Stratmann, The delamination of polymeric coatings from steel Part 3: Effect of the oxygen partial pressure on the delamination reaction and current distribution at the metal/polymer interface, Corros. Sci. 41 (1998) 599–620, https://doi.org/10.1016/S0010-938X(98)00168-1.
[4] M. Stratmann, R. Feser, A. Leng, Corrosion protection by organic films, Electrochim. Acta 39 (1994) 1207–1214, https://doi.org/10.1016/0013-4686(94)E0038-2.
[5] B. Salgin, D. Vogel, D. Pontoni, H. Schröder, B. Schönberger, M. Stratmann, H. Reichert, M. Rohwerder, A scanning Kelvin probe for synchrotron investigations: the in situ detection of radiation-induced potential changes, J. Synchrotron Radiat. 19 (2012) 48–53, https://doi.org/10.1107/S0909049511047066.
[6] B. Salgin, R.F. Hamou, M. Rohwerder, Monitoring surface ion mobility on aluminum oxide: effect of chemical pretreatments, Electrochim. Acta 110 (2013) 526–533, https://doi.org/10.1016/j.electacta.2013.03.060.
[7] N.V. Mandich, D.L. Snyder, Electrodeposition of chromium, in: M.P. Mordechay Schlesinger (Ed.), Mod. Electroplat., 5th ed., John Wiley & Sons, Inc., Hoboken, NJ, USA, 2011, pp. 205–248, https://doi.org/10.1002/9780470602638.ch7.
[8] T. Petry, R. Knowles, R. Meads, An analysis of the proposed REACH regulation, Regul. Toxicol. Pharmacol. 44 (2006) 24–32, https://doi.org/10.1016/j.yrtph.2005.07.007.
[9] J.M. Prabhakar, R.S. Varanasi, C.C. da Silva, A. Saba, A. de Vooys, M. Erbe, Rohwerder, Chromium coatings from trivalent chromium plating baths: characterization and cathodic delamination behaviour, Corros. Sci. 187 (2021), 109525, https://doi.org/10.1016/j.corsci.2021.109525.
[10] J.E. Edy, H.N. McMurray, K.R. Lammers, A.C.A. deVooys, Kinetics of corrosion-driven cathodic disbondment on organic coated trivalent chromium metal-oxide-carbide coatings on steel, Corros. Sci. 157 (2019) 51–61, https://doi.org/10.1016/j.corsci.2019.04.037.
[11] N. Wint, A.C.A.C.A. de Vooys, H.N.N. McMurray, The corrosion of chromium based coatings for packaging steel, Electrochim. Acta 203 (2016) 326–336, https://doi.org/10.1016/j.electacta.2016.01.100.
[12] C. Melvin, E. Jewell, A. de Vooys, K. Lammers, N.M. Murray, Surface and adhesion characteristics of current and next generation steel packaging materials, J. Packag. Technol. Res. 2 (2018) 93–103, https://doi.org/10.1007/s41783-018-0031-8.
[13] G. Grundmeier, W. Schmidt, M. Stratmann, Corrosion protection by organic coatings: electrochemical mechanism and novel methods of investigation, Electrochim. Acta 45 (2000) 2515–2533, https://doi.org/10.1016/S0013-4686(00)00348-0.
[14] H.N. McMurray, G. Williams, Under film/coating corrosion, in: Shreir's Corros., Elsevier, 2010, pp. 988–1004, https://doi.org/10.1016/B978-044452787-5.00040-8.
[15] D. Iqbal, R.S. Moirangthemy, A. Bashir, A. Erbe, Study of polymer coating delamination kinetics on zinc modified with zinc oxide of different morphologies, Mater. Corros. 65 (2014) 370–375, https://doi.org/10.1002/maco.201307533.
[16] M. Uebel, L. Exbrayat, M. Rabe, T.H. Tran, D. Crespy, M. Rohwerder, On the role of trigger signal spreading velocity for efficient self-healing coatings for corrosion protection, J. Electrochem. Soc. 165 (2018) C1017–C1027, https://doi.org/10.1149/2.0811816jes.
[17] S. Salaluk, S. Jiang, E. Viyanit, M. Rohwerder, K. Landfester, D. Crespy, Design of nanostructured protective coatings with a sensing function, ACS Appl. Mater. Interfaces 13 (2021) 53046–53054, https://doi.org/10.1021/acsami.1c14110.
[18] M. Stratmann, M. Wolpers, H. Streckel, R. Feser, Use of a scanning-Kelvinprobe in the investigation of electrochemical reactions at the metal/polymer interface, Ber. Bunsenges. Phys. Chem. 95 (1991) 1365–1375, https://doi.org/10.1002/bbpc.19910951109.
[19] M. Stratmann, H. Streckel, R. Feser, A new technique able to measure directly the delamination of organic polymer films, Corros. Sci. 32 (1991) 467–470, https://doi.org/10.1016/0010-938X(91)90126-A.
[20] K. Hoffmann, M. Stratmann, The delamination of organic coatings from rusty steel substrates, Corros. Sci. 34 (1993) 1625–1645, https://doi.org/10.1016/0010-938X(93)90037-H.
[21] W. Fürbeth, M. Stratmann, Investigation of the delamination of polymer films from galvanized steel with the Scanning Kelvinprobe, Fresenius, J. Anal. Chem. 353 (1995) 337–341, https://doi.org/10.1007/BF00322064.
[22] M. Stratmann, A. Leng, W. Fürbeth, H. Streckel, H. Gehmecker, K.-H. Große-Brinkhaus, The scanning Kelvin probe; a new technique for the in situ analysis of the delamination of organic coatings, Prog. Org. Coat. 27 (1996) 261–267, https://doi.org/10.1016/0300-9440(94)00542-7.
[23] A. Leng, H. Streckel, M. Stratmann, The delamination of polymeric coatings from steel. Part 1: calibration of the Kelvinprobe and basic delamination mechanism, Corros. Sci. 41 (1998) 547–578, https://doi.org/10.1016/S0010-938X(98)00166-8.
[24] A. Leng, H. Streckel, M. Stratmann, The delamination of polymeric coatings from steel. Part 2: first stage of delamination, effect of type and concentration of cations on delamination, chemical analysis of the interface, Corros. Sci. 41 (1998) 579–597, https://doi.org/10.1016/S0010-938X(98)00167-X.
[25] M. Stratmann, H. Streckel, On the atmospheric corrosion of metals which are covered with thin electrolyte layers—I. Verification of the experimental technique, Corros. Sci. 30 (1990) 681–696, https://doi.org/10.1016/0010-938X(90)90032-Z.
[26] M. Rohwerder, F. Turcu, High-resolution Kelvin probe microscopy in corrosion science: scanning Kelvin probe force microscopy (SKPFM) versus classical scanning Kelvin probe (SKP), Electrochim. Acta 53 (2007) 290–299, https://doi.org/10.1016/j.electacta.2007.03.016.
[27] R. Hausbrand, M. Stratmann, M. Rohwerder, Delamination resistant zinc alloys: simple concept and results on the system zinc-magnesium, Steel Res. Int. 74 (2003) 453–458, https://doi.org/10.1002/srin.200300212.
[28] W. Fürbeth, M. Stratmann, Scanning Kelvin Probe investigations on the delamination of polymeric coatings from metallic surfaces, Prog. Org. Coat. 39 (2000) 23–29, https://doi.org/10.1016/S0300-9440(00)00095-3.

[29] W. Fürbeth, M. Stratmann, The delamination of polymeric coatings from electrogalvanized steel – a mechanistic approach. Part 3: delamination kinetics and influence of CO_2, Corros. Sci. 43 (2001) 243–254, https://doi.org/10.1016/S0010-938X(00)00049-4.
[30] V. Shkirskiy, M. Uebel, A. Maltseva, G. Lefèvre, P. Volovitch, M. Rohwerder, Cathodic driven coating delamination suppressed by inhibition of cation migration along Zn|polymer interface in atmospheric CO_2, Npj Mater. Degrad. 3 (2019) 1–10, https://doi.org/10.1038/s41529-018-0064-z.
[31] Z.Y. Chen, D. Persson, A. Nazarov, S. Zakipour, D. Thierry, C. Leygraf, In situ studies of the effect of CO_2 on the initial NaCl-induced atmospheric corrosion of copper, J. Electrochem. Soc. 152 (2005) B342, https://doi.org/10.1149/1.1984448.
[32] J. Sitte, Relation between reference levels, work functions and contact potential differences in photoelectron spectroscopy, Chem. Phys. Lett. 42 (1976) 131–132, https://doi.org/10.1016/0009-2614(76)80568-4.
[33] O.I. Klyushnikov, Method to determine the work function using X-ray Photoelectron Spectroscopy, J. Struct. Chem. 39 (1998) 944–947.
[34] M. Uebel, A. Vimalanandan, A. Laaboudi, S. Evers, M. Stratmann, D. Diesing, M. Rohwerder, Fabrication of robust reference tips and reference electrodes for Kelvin probe applications in changing atmospheres, Langmuir 33 (2017) 10807–10817, https://doi.org/10.1021/acs.langmuir.7b02533.
[35] G.S. Frankel, M. Stratmann, M. Rohwerder, A. Michalik, B. Maier, J. Dora, M. Wicinski, Potential control under thin aqueous layers using a Kelvin Probe, Corros. Sci. 49 (2007) 2021–2036, https://doi.org/10.1016/j.corsci.2006.10.017.
[36] R. Hausbrand, M. Stratmann, M. Rohwerder, The physical meaning of electrode potentials at metal surfaces and polymer/metal interfaces: consequences for delamination, J. Electrochem. Soc. 155 (2008) C369, https://doi.org/10.1149/1.2926589.
[37] M. Rohwerder, Passivity of Metals and the Kelvin Probe Technique, Elsevier Inc., 2018, https://doi.org/10.1016/B978-0-12-409547-2.13405-5.
[38] R. Posner, T. Titz, K. Wapner, M. Stratmann, G. Grundmeier, Transport processes of hydrated ions at polymer/oxide/metal interfaces. Part 2. Transport on oxide covered iron and zinc surfaces, Electrochim. Acta 54 (2009) 900–908, https://doi.org/10.1016/j.electacta.2008.07.011.
[39] T.G. Avval, S. Chatterjee, S. Bahr, P. Dietrich, M. Meyer, A. Thißen, M.R. Linford, Carbon dioxide gas, CO 2 (g), by near-ambient pressure XPS, Surf. Sci. Spectra 26 (2019), 014022, https://doi.org/10.1116/1.5053761.
[40] T.G. Avval, S. Chatterjee, G.T. Hodges, S. Bahr, P. Dietrich, M. Meyer, A. Thißen, M. R. Linford, Oxygen gas, O 2 (g), by near-ambient pressure XPS, Surf. Sci. Spectra 26 (2019), 014021, https://doi.org/10.1116/1.5100962.
[41] J. Hedman, P.F. Hedén, C. Nordling, K. Siegbahn, Energy splitting of core electron levels in paramagnetic molecules, Phys. Lett. A 29 (1969) 178–179, https://doi.org/10.1016/0375-9601(69)90801-9.
[42] A.P. Nazarov, D. Thierry, Scanning Kelvin probe study of metal/polymer interfaces, Electrochim. Acta 49 (2004) 2955–2964, https://doi.org/10.1016/j.electacta.2004.01.054.
[43] J. Wielant, R. Posner, G. Grundmeier, H. Terryn, Interface dipoles observed after adsorption of model compounds on iron oxide films: effect of organic functionality and oxide surface chemistry, J. Phys. Chem. C 112 (2008) 12951–12957, https://doi.org/10.1021/jp802703v.
[44] S. Porsgaard, P. Jiang, F. Borondics, S. Wendt, Z. Liu, H. Bluhm, F. Besenbacher, M. Salmeron, Charge state of gold nanoparticles supported on titania under oxygen pressure, Angew. Chem. Int. Ed. 50 (2011) 2266–2269, https://doi.org/10.1002/anie.201005377.
[45] G. Pirug, G. Brodén, H.P. Bonzel, Coadsorption of potassium and oxygen on Fe (110), Surf. Sci. 94 (1980) 323–338, https://doi.org/10.1016/0039-6028(80)90010-2.
[46] A.F. Carley, S. Rassias, M.W. Roberts, The specificity of surface oxygen in the activation of adsorbed water at metal surfaces, Surf. Sci. 135 (1983) 35–51, https://doi.org/10.1016/0039-6028(83)90208-X.
[47] W. Kuch, M. Schulze, W. Schnurnberger, K. Bolwin, XPS lineshape analysis of potassium coadsorbed with water on Ni(111), Surf. Sci. 287–288 (1993) 600–604, https://doi.org/10.1016/0039-6028(93)91035-N.
[48] C. Benndorf, C. Nöbl, F. Thieme, Interaction of H2O with a clean and oxygen precovered Ni(110) surface studied by XPS, Surf. Sci. 121 (1982) 249–259, https://doi.org/10.1016/0039-6028(82)90041-3.
[49] N. Cabrera, N.F. Mott, Theory of the oxidation of metals, Rep. Prog. Phys. 12 (1949) 308, https://doi.org/10.1088/0034-4885/12/1/308.
[50] V.F. Kiselev, O.V. Krylov. Adsorption and Catalysis on Transition Metals and Their Oxides, Springer Berlin Heidelberg, Berlin, Heidelberg, 1989, https://doi.org/10.1007/978-3-642-73887-6.
[51] H.H. Kung, Chapter 2 Bulk and surface structure of transition metal oxide, in: Stud, Surf. Sci. Catal. (1989) 6–26. https://doi.org/10.1016/S0167-2991(08)60925-8.
[52] M.T. Greiner, Z.H. Lu, Thin-film metal oxides in organic semiconductor devices: their electronic structures, work functions and interfaces, NPG Asia Mater. 5 (2013) 1–16, https://doi.org/10.1038/am.2013.29.
[53] Z. Zhang, J.T. Yates, Band bending in semiconductors: chemical and physical consequences at surfaces and interfaces, Chem. Rev. 112 (2012) 5520–5551, https://doi.org/10.1021/cr3000626.
[54] Z. Zhang, J.T. Yates, Effect of adsorbed donor and acceptor molecules on electron stimulated desorption: O2/TiO2(110), J. Phys. Chem. Lett. 1 (2010) 2185–2188, https://doi.org/10.1021/jz1007559.
[55] Z. Zhang, J.T. Yates, Electron-mediated co oxidation on the TiO2(110) surface during electronic excitation, J. Am. Chem. Soc. 132 (2010) 12804–12807, https://doi.org/10.1021/ja106207w.
[56] Y. Gao, Surface analytical studies of interfaces in organic semiconductor devices, Mater. Sci. Eng. R. Rep. 68 (2010) 39–87, https://doi.org/10.1016/j.mser.2010.01.001.
[57] R. Krieg, M. Rohwerder, S. Evers, B. Schuhmacher, J. Schauer-Pass, Cathodic self-healing at cut-edges: the effect of Zn^{2+} and Mg^{2+} ions, Corros. Sci. 65 (2012) 119–127, https://doi.org/10.1016/j.corsci.2012.08.008.
[58] C. Senöz, S. Borodin, M. Stratmann, M. Rohwerder, In situ detection of differences in the electrochemical activity of Al_2Cu IMPs and investigation of their effect on FFC by scanning Kelvin probe force microscopy, Corros. Sci. 58 (2012) 307–314, https://doi.org/10.1016/j.corsci.2012.02.006.
[59] K. Wapner, M. Stratmann, G. Grundmeier, In situ infrared spectroscopic and scanning Kelvin probe measurements of water and ion transport at polymer/metal interfaces, Electrochim. Acta 51 (2006) 3303–3315, https://doi.org/10.1016/j.electacta.2005.09.024.